



Production of the W and Z bosons in the nucleon–(anti)nucleon collisions and the meson cloud in the nucleon

A. Szczurek^a, V. Uleshchenko^a, H. Holtmann^b, J. Speth^b

^a *Institute of Nuclear Physics, ul. Radzikowskiego 152, PL-31-342 Kraków, Poland*

^b *Institut für Kernphysik, Forschungszentrum, D-52425 Jülich, Germany*

Received 21 March 1997; revised 10 June 1997

Abstract

We investigate possible consequences of the meson cloud in the nucleon for the production of the W and Z bosons in hadron–hadron collisions. We start from the description of the muon and charged-current (anti)neutrino deep-inelastic scattering. We get a good description of the total W and Z production cross sections measured in the proton–antiproton collisions by the UA1 and UA2 Collaborations at CERN and the CDF Collaboration at FNAL as well as the lepton asymmetry obtained recently by the CDF Collaboration. Our model predicts an enhancement of the cross section for the W boson production in proton–proton collisions in comparison to proton–antiproton collisions. The charge lepton asymmetry measured recently by the CDF Collaboration can be described only if meson cloud effects are included explicitly. We critically study a possibility to test the $\bar{d}-\bar{u}$ asymmetry in the nucleon by the analysis of various asymmetries possible to measure in principle at RHIC. © 1997 Elsevier Science B.V.

PACS: 13.38.Be; 13.38.Dg; 14.20.Dh

1. Introduction

Good quality experimental data for both unpolarized and polarized deep inelastic scattering collected over last ten years by BCDMS, EMC, NMC and CCFR Collaborations has opened an interesting possibility to study in much greater detail than before the internal structure of the nucleon. Some of those results have demonstrated that the nucleon structure is more complicated than it was previously expected.

In particular, the deviation of the Gottfried Sum Rule (GSR) from its classical value [1]

$$S_G = \int_0^1 [F_2^p(x) - F_2^n(x)] \frac{dx}{x} = \frac{1}{3} \quad (1)$$

observed by the New Muon Collaboration (NMC) at CERN [2,3] ($S_G = 0.235 \pm 0.026$) has created a lot of interest in the possible sources of its violation.

It is commonly believed at present that this violation is a consequence of an internal asymmetry of the $\bar{d}(x)$ and $\bar{u}(x)$ quark distributions in the proton (the opposite asymmetry is expected for the neutron if the proton–neutron charge symmetry holds). A recent CERN experiment [4] on the production of dileptons in proton–proton and proton–deuteron collisions is consistent with such an assumption.

Since to leading order in $\log Q^2$ the perturbative QCD evolution is flavour independent and generates an equal number of $\bar{u}u$ and $\bar{d}d$ sea quarks [5,6] it is natural to expect that non-perturbative effects must be responsible for the effect. It was suggested already long ago by Field and Feynman [7] that the Pauli blocking effect could lead to some asymmetry in $\bar{u}(x)$ and $\bar{d}(x)$ distributions. Since then the idea was almost completely forgotten. Only recently this idea was used to construct phenomenological quark distributions [8] with parameters adjusted to describe the Gottfried sum rule violation. Parallel the \bar{u} – \bar{d} asymmetry has been predicted by meson cloud models in which the physical nucleon contains an admixture of the πN and $\pi \Delta$, etc. components in the Fock expansion [9]. This forty year old idea got in the last decade a lot of theoretical support by constructors of the nucleon structure based on chiral symmetry and spontaneous chiral symmetry breaking arguments. The idea of meson cloud and Pauli blocking are not contradictory. In fact, the meson cloud effect can be viewed as a dynamical many-body (multi-quark) realization of the Pauli blocking principle. It has only recently been shown that such a model is consistent with the violation of the Gottfried Sum Rule [10], the production of the dimuon pairs in the high energy Drell–Yan processes [11,12] and some hadronic semi-inclusive processes [10]. In particular, it provides the only known to us explanation of the asymmetry measured by the NA51 CERN experiment on Drell–Yan processes [4]. The presence of the meson cloud in the nucleon offers a possibility to understand scaling violation of the electromagnetic form factors [13].

It is the aim of this work to study possible consequences of the meson cloud for the W and Z weak gauge boson production in the nucleon–(anti)nucleon collisions. We start our analysis with the description of the deep inelastic structure functions. Then we confront the prediction of the meson cloud model with the existing CERN and FNAL experimental data on the production of W and Z bosons in the $p + \bar{p}$ collisions. It was suggested recently [14] that the analysis of the W production in the proton–proton and proton–deuteron reactions could give a valuable information on the asymmetry of the nucleon sea. We analyze this problem in detail and make predictions based on the quark distributions calculated in the framework of our model, where the \bar{d} – \bar{u} asymmetry results from the effects of the meson cloud.

2. Meson cloud model of the nucleon and lepton deep inelastic scattering

In this section we briefly sketch the meson cloud model (MCM) of the nucleon [10] and confront its predictions with some selected deep inelastic data. In this model the nucleon is viewed as a quark core, termed a bare nucleon, “surrounded” by the mesonic cloud. The nucleon wave function can be schematically written as a superposition of a few principle Fock components (only πN and $\pi \Delta$ components are shown explicitly)

$$\begin{aligned}
 |p\rangle_{\text{phys}} = \sqrt{Z} & \left[|p\rangle_{\text{core}} + \int dy d^2 \mathbf{k}_{\perp} \phi_{N\pi}(y, \mathbf{k}_{\perp}) \left(\sqrt{\frac{1}{3}} |p\pi^0; y, \mathbf{k}_{\perp}\rangle + \sqrt{\frac{2}{3}} |n\pi^+; y, \mathbf{k}_{\perp}\rangle \right) \right. \\
 & + \int dy d^2 \mathbf{k}_{\perp} \phi_{\Delta\pi}(y, \mathbf{k}_{\perp}) \\
 & \times \left. \left(\sqrt{\frac{1}{2}} |\Delta^{++}\pi^-; y, \mathbf{k}_{\perp}\rangle - \sqrt{\frac{1}{3}} |\Delta^+\pi^0; y, \mathbf{k}_{\perp}\rangle + \sqrt{\frac{1}{6}} |\Delta^0\pi^+; y, \mathbf{k}_{\perp}\rangle \right) + \dots \right].
 \end{aligned} \quad (2)$$

with Z being the wave function renormalization constant which can be calculated by imposing the normalization condition $\langle p|p\rangle = 1$. The $\phi(y, \mathbf{k}_{\perp})$'s are the light cone wave functions of the πN , $\pi \Delta$, etc. Fock states, y is the longitudinal momentum fraction of the π (meson) and \mathbf{k}_{\perp} its transverse momentum.

It can be expected that the structure of the bare nucleon (core) is rather simple. Presumably, it can be described as a three quark system in the static limit. Of course, in deep inelastic scattering regime at higher Q^2 an additional sea of perturbative nature is created unavoidably by the standard QCD evolution equations.

The model includes all the mesons and baryons required in the description of the low energy nucleon–nucleon and hyperon–nucleon scattering, i.e. π , K , ρ , ω , K^* and N , Λ , Σ , Δ and Σ^* . In contrast to other approaches in the literature the model ensures charge conservation, baryon number and momentum sum rules [10] by construction.

The main ingredients of the model are the vertex coupling constants, the parton distribution functions for the virtual mesons and baryons and the vertex form factors which account for the extended nature of the hadrons. The coupling constants are assumed to be related via $SU(3)$ symmetry which seems to be well established from low-energy hyperon–nucleon scattering.

It was suggested in Ref. [15] to use the light cone meson–baryon vertex form factor

$$F(y, k_{\perp}^2) = \exp \left[-\frac{(M_{\text{MB}}^2(y, k_{\perp}^2) - m_N^2)}{2\Lambda_{\text{MB}}^2} \right], \quad (3)$$

where \mathbf{k}_{\perp} is the transverse momentum of the meson and $M_{\text{MB}}(y, k_{\perp}^2)$ is the invariant mass of the intermediate two-body meson–baryon Fock state,

$$M_{\text{MB}}^2(y, k_{\perp}^2) = \frac{m_B^2 + k_{\perp}^2}{1-y} + \frac{m_M^2 + k_{\perp}^2}{y}. \quad (4)$$

By construction, such form factors assure the momentum sum rule [15,10]. The parameters A_{MB} are the principal non-perturbative parameters of the model. They have been determined from an analysis of the $p \rightarrow n, \Delta, \Lambda$, fragmentation spectra [10] using the light cone flux functions [10] ($A_{\pi N}^2 = 1.08 \text{ GeV}^2$ and $A_{\pi \Delta}^2 = 0.98 \text{ GeV}^2$). With these parameters the pion exchange model gives a good description of the energy spectra of baryons.

The x dependence of the structure functions can be written as a sum of components corresponding to the expansion given by Eq. (2).

$$F_2^N(x) = Z \left[F_{2,\text{core}}^N(x) + \sum_{\text{MB}} (\delta^{(\text{M})} F_2^N(x) + \delta^{(\text{B})} F_2^N(x)) \right]. \quad (5)$$

The contributions from the virtual mesons can be written as a convolution of the meson structure functions and its longitudinal momentum distribution in the nucleon [16]

$$\delta^{(\text{M})} F_2(x) = \int_x^1 dy f_{\text{M}}(y) F_2^{\text{M}}\left(\frac{x}{y}\right). \quad (6)$$

The same is true for the bare baryon component

$$\delta^{(\text{B})} F_2(x) = \int_x^1 dy f_{\text{B}}(y) F_{2,\text{core}}^{\text{B}}\left(\frac{x}{y}\right). \quad (7)$$

In the light-cone approach $f_{\text{M}}(y)$ and $f_{\text{B}}(y)$ are related via [10]

$$f_{\text{B}}(y) = f_{\text{M}}(1-y). \quad (8)$$

Eq. (6) (and also Eq. (7)) can be written in an equivalent form in terms of the quark distribution functions

$$\delta^{(\text{M})} q_{\text{f}}(x) = \int_x^1 f_{\text{M}}(y) q_{\text{f}}^{\text{M}}\left(\frac{x}{y}\right) \frac{dy}{y}. \quad (9)$$

The longitudinal momentum distributions (splitting functions, flux factors) of virtual mesons (or baryons) can be calculated assuming a model of the vertex and depend on the coupling constants and vertex form factors. Further details can be found in Refs. [10].

The parton distributions “measured” in pion-nucleus Drell–Yan processes [17] are used for the mesons. The deep-inelastic structure functions of the bare baryons $F_{2,\text{core}}^N(x, Q^2)$ and $F_{2,\text{core}}^B(x, Q^2)$ are in principle unknown. In practical calculations it is usually assumed $F_{2,\text{core}}^N(x, Q^2) = F_{2,\text{phys}}^N(x, Q^2)$ [18], which is not fully consistent. Recently [12], we have extracted $F_{2,\text{core}}^N$ by fitting the quark distributions in the bare nucleon, together with (parameter-free) mesonic corrections, to the experimental data on deep-inelastic scattering. In comparison to Ref. [12] a somewhat more flexible form of the sea quark distributions in the bare nucleon (baryon) has been used in the

present paper. In the following we shall deal both with small and large x at relatively small Q^2 , where the target mass corrections may play important role. In this region the Bjorken- x cannot be interpreted as a longitudinal momentum fraction of the nucleon carried by a parton. In general the target mass corrections is a complicated [19,20] and not fully explored area. In the present paper we include the most important kinematical effect and replace the measured Bjorken- x by the target mass variable ξ often called the Nachtmann variable

$$\xi = \frac{2x}{1+r} \quad \text{with} \quad r^2 = 1 + \frac{4M_N^2 x^2}{Q^2}. \quad (10)$$

By construction, the variable $\xi \rightarrow x$ in the Bjorken limit $Q^2 \rightarrow \infty$. This idea was often used in the past by experimental groups to “correct” structure functions in the large- x region. It was demonstrated in Ref. [21] that this kinematical correction gives a dramatic improvement in the description of the large- x DIS data. In order to fix the parameters of the bare nucleon we have used the following sets of DIS data:

- (a) $F_2^d(x, Q^2)$ [3],
- (b) $F_2^p(x, Q^2) - F_2^n(x, Q^2)$ [3],
- (c) $F_2^n(x, Q^2)/F_2^p(x, Q^2)$ [3],
- (d) $F_3^{\nu N}(x, Q^2)$ [22].

In comparison to Ref. [12] we have replaced in the fit the sea quark distributions from Ref. [23] by the deep inelastic structure function of the deuteron. We have found that it is impossible to fit simultaneously both, especially at small- x , which seems to suggest incompatibility of these two experimental data sets. While the previous is obtained as a difference of $F_2^{\nu N}(x)$ and $F_3^{\nu N}(x)$ [23], the latter is known fairly precisely.

The following simple parameterization has been used for the quark distributions in the bare proton at the initial scale $Q_0^2 = 4 \text{ (GeV}/c)^2$.

$$xu_{v,\text{core}}(x) = A_u x^{\alpha_u} (1-x)^{\beta_u} (1 + \gamma_u x), \quad (11)$$

$$xd_{v,\text{core}}(x) = A_d x^{\alpha_d} (1-x)^{\beta_d} (1 + \gamma_d x), \quad (12)$$

$$xS_{\text{core}}(x) = A_S (1-x)^{\eta_S} (1 + \gamma_S x), \quad (13)$$

$$xg_{\text{core}}(x) = A_g x^{\alpha_g} (1-x)^{\beta_g}. \quad (14)$$

Note, that we have used $SU(2)$ symmetric sea quark distribution for the bare baryons and suppressed the strange sea distributions by a factor 2 as known from the (anti)neutrino induced DIS [24]

$$S_{\text{core}} = u_{s,\text{core}} = \bar{u}_{s,\text{core}} = d_{s,\text{core}} = \bar{d}_{s,\text{core}} = 2s_{s,\text{core}} = 2\bar{s}_{s,\text{core}}. \quad (15)$$

The leading order analysis of selected DIS data does not allow to constrain very well the gluon distribution in the nucleon. For this purpose one can try to fit the gluon distribution by the analysis of large p_T direct photon production data. Although the prompt photon

Table 1

The parameters of the bare nucleon quark distributions (14) found from the fit to the DIS data

Fit	α_u	β_u	γ_u	α_d	β_d	γ_d	A_S	η_S	γ_S
1 meson cloud, no TMC	0.404	2.54	9.43	0.111	4.35	66.2	0.201	12.2	0.334
2 no meson cloud, no TMC	0.383	2.62	3.94	0.363	5.91	26.0	0.255	5.45	0.001
3 meson cloud, with TMC	0.237	2.99	32.9	0.053	4.27	173	0.217	15.6	0.625
4 no meson cloud, with TMC	0.266	3.35	13.5	0.516	5.52	9.39	0.277	8.56	0.034

data provide a direct measurement of the gluon distribution, the available data have still large point-to-point and overall normalization errors. On the theoretical side there is a strong dependence on both factorization and renormalization scale assumed. We have checked that quite different gluon distributions cannot be excluded by a comparison to the data. In the following for simplicity we shall keep $\alpha_g = 0$ and $\beta_g = 5.3$. The exponent $\beta_g = 5.3$ has been taken the same as in Ref. [25] where it was fitted to a large body of experimental data. The normalization of the gluon distribution is obtained here as usual through the momentum sum rule. As will be discussed later, the observables discussed in the present paper are practically insensitive to a detailed shape of the gluon distribution.

A typical fit to the data is shown in Fig. 1. The solid line corresponds to the fit, hereafter called “Model 1” for brevity, which explicitly includes the meson cloud corrections. For comparison by the dashed line we show also a result without meson cloud correction called “Model 2” in the present paper. The parameters of parametrization (14) corresponding to the fit shown in Fig. 1 are collected in Table 1. For comparison we present also parameters of the fit where the target mass corrections (TMC) have been omitted. For completeness in Fig. 2 we show the result for $x\bar{q}(x)$ together with experimental data from Ref. [23], which was used in Ref. [12] to constrain the fit parameters.

Up to now it was proven only how to include consistently the meson cloud corrections together with leading-order (LO) QCD effects. It should become clear that a consistent next-to-leading order (NLO) analysis goes beyond the scope of the present paper. Needless to say that such an analysis will be rather difficult and cumbersome. The effect of the NLO corrections on the cross sections for the production of gauge bosons will be discussed below.

The existence of the meson cloud in the nucleon leads to a special flavour and valence/sea structure of parton distributions [10]. Therefore it seems interesting to compare the quark distributions obtained here with recent NLO global fits to broad range of hard scattering data [25–27]. It is not obvious a priori that the special structure can be accommodated in simple power-like parametrizations used in the literature. We wish to emphasize that there are some quantities which are independent of quark distributions in the bare nucleon (14) and are true (parameter-free) predictions of the meson cloud model. Some of them have been discussed in Ref. [12]. In particular, the meson cloud effects allow to explain the x -dependence of the difference $\bar{d}-\bar{u}$ fitted in Ref. [25–27].

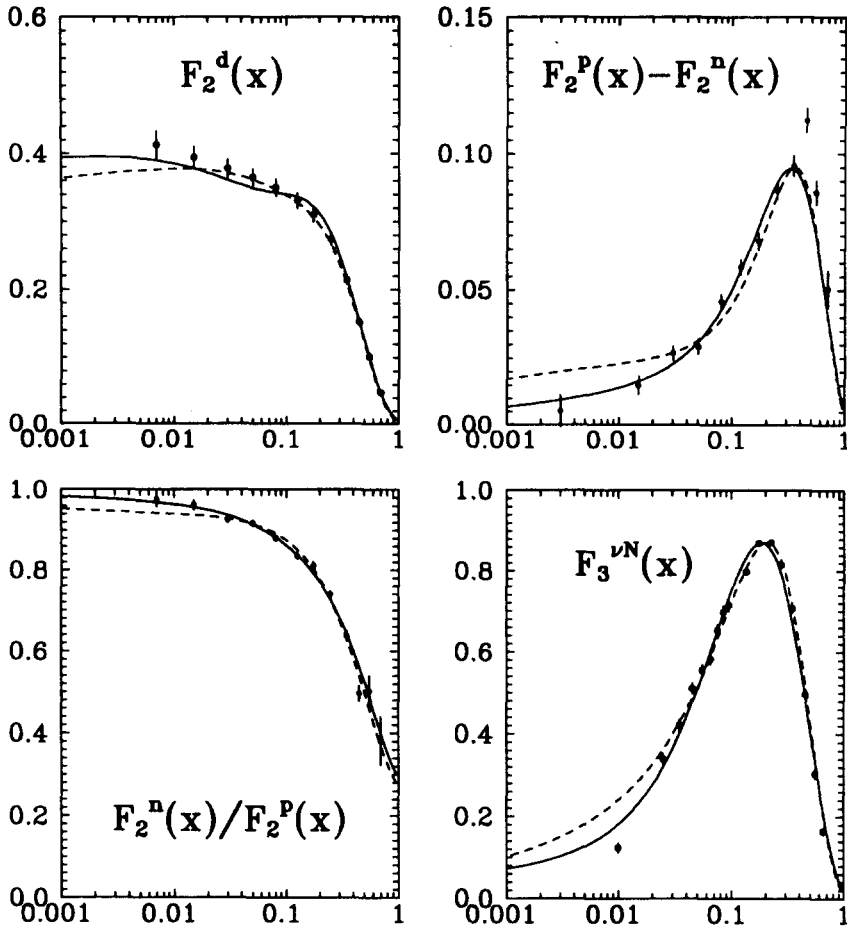


Fig. 1. The deep-inelastic scattering data. The solid line corresponds to the fit which explicitly includes the meson cloud corrections. For comparison we show result without meson cloud corrections (dashed line). (a) $F_2^d(x)$, (b) $F_2^p(x) - F_2^n(x)$, (c) $F_2^n(x)/F_2^p(x)$, (d) $F_3^{\nu N}(x)$.

The obtained agreement between our predictions and the result of the global fits [25] can be viewed as an explanation of pure fits as well as an indirect confirmation of the non-perturbative picture of the nucleon. Although the pion cloud contributes to both valence and sea quark distributions, in general the valence quark distributions obtained in the present approach are rather similar to those obtained from pure fits.

In contrast to fits our model provides an interesting predictions in many branches of “soft” and “hard” physics. For example our model predicts an unique energy dependence of outgoing neutrons produced in hard collisions at HERA, which has been verified recently by the ZEUS Collaboration [28], while standard hadronization models are not able to explain the observed energy dependence. ¹

¹ After this paper has been completed it has been found that the quark distributions obtained here, with the inclusion of the target mass corrections and the meson cloud effects, lead to a sizeable and desirable enhancement of the large- E_T jet cross section [29] observed recently by the CDF Collaboration [30].

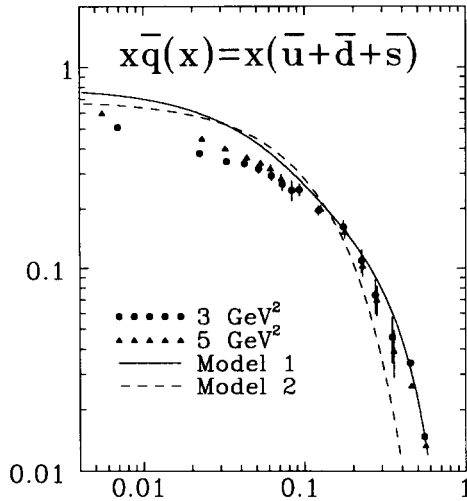


Fig. 2. $x\bar{q}(x)$ calculated in our Model 1 (solid line) and Model 2 (dashed line) compared with the results extracted from deep-inelastic (anti)neutrino scattering off nucleons [23].

3. Production of W and Z bosons in the nucleon–anti(nucleon) collisions

In last years a significant progress has been achieved in calculating next-to-leading order QCD corrections for the production of gauge bosons [31]. The NLO calculations turned out to be extremely important in understanding the difference between the magnitude of the cross section predicted by LO calculation and the experimental data. Our primary aim in the present paper is to demonstrate a simple relation between the non-perturbative effect of the meson cloud and the production of the W/Z bosons in the nucleon–(anti)nucleon collisions. It is known that to a good approximation the effect of the NLO corrections can be accounted for by introducing so-called K -factors to leading order results. While sufficient for the total cross section it may become insufficient for differential distributions. In the following we shall try to select quantities which are expected to be insensitive to the NLO corrections. The accuracy of the LO approximation will be discussed in the next section.

In the leading order (LO) approximation in the framework of improved parton model [32] the total $B(=W^\pm, Z^0)$ boson cross section is the convolution of elementary cross section $\hat{\sigma}(q\bar{q}' \rightarrow B)$ with the quark densities

$$\begin{aligned} \sigma(h_1 h_2 \rightarrow BX) = & \frac{K}{3} \int_0^1 dx_1 dx_2 \sum_{q, q'} [q(x_1, M_B^2) \bar{q}'(x_2, M_B^2) \hat{\sigma}(q\bar{q}' \rightarrow B) \\ & + \bar{q}'(x_1, M_B^2) q(x_2, M_B^2) \hat{\sigma}(\bar{q}'q \rightarrow B)]. \end{aligned} \quad (16)$$

In analogy to the Drell–Yan processes the so-called K -factor in Eq. (16) includes first order QCD corrections due to a difference between space-like (DIS) and time-like (Drell–Yan, here) Q^2 . Its value can be easily calculated (see for instance [32]).

$$K = 1 + \frac{\alpha_s(M_B^2)}{2\pi} \frac{4}{3} \left(1 + \frac{4}{3} \pi^2 \right) \approx 1 + \frac{8\pi}{9} \alpha_s(M_B^2). \quad (17)$$

In the leading order approximation the strong coupling constant

$$\alpha_s(Q^2) = \frac{12\pi}{33 - 2n_f \log \left(Q^2 / (\Lambda_{\text{QCD}}^{(n_f)})^2 \right)}, \quad (18)$$

where n_f is the number of active flavours. The elementary cross sections can be easily calculated within Standard Model

$$\begin{aligned} \hat{\sigma}(q\bar{q}' \rightarrow W^\pm) &= 2\pi \frac{G_F}{\sqrt{2}} |V_{qq'}|^2 \frac{\Gamma_W M_W}{\pi} \frac{\hat{s}}{(\hat{s} - M_W^2)^2 + (\Gamma_W M_W)^2}, \\ \hat{\sigma}(q\bar{q}' \rightarrow Z^0) &= 8\pi \frac{G_F}{\sqrt{2}} [(g_V^q)^2 + (g_A^q)^2] \frac{\Gamma_Z M_Z}{\pi} \frac{\hat{s}}{(\hat{s} - M_Z^2)^2 + (\Gamma_Z M_Z)^2} \delta_{qq'}. \end{aligned} \quad (19)$$

The $V_{qq'}$ matrix represents the familiar Cabibbo–Kobayashi–Maskawa (CKM) matrix which is rather well known at present [33]. The vector and axial-vector quark- Z^0 coupling constants can be expressed by a weak isospin and charge of the quark $g_V^q = \frac{1}{2}T_3^q - Q^q x_W$, $g_A^q = -\frac{1}{2}T_3^q$ and $x_W \equiv \sin^2 \theta_W$ ($x_W = 0.2325$ [33]). The sum in Eq. (16) is limited by the charge conservation $e_q + e_{\bar{q}} = \pm 1$ for W^\pm and $e_q + e_{\bar{q}'} = 0$ for Z^0 .

Let us consider now a rapidity distribution of the gauge boson produced in the $h_1 + h_2$ collisions. The double integration over x_1, x_2 in Eq. (16) can be reduced by making variable transformation $dx_1 dx_2 \rightarrow d\hat{s} dy_B$ and the following sharp (“ δ -like”) B -resonance approximation:

$$\frac{\hat{s}}{(\hat{s} - M_B^2)^2 + (\Gamma_B M_B)^2} \rightarrow \frac{\pi M_B}{\Gamma_B} \delta(\hat{s} - M_B^2). \quad (20)$$

Then the rapidity distribution of W^\pm boson produced in the $h_1 + h_2$ collision is

$$\begin{aligned} \frac{d\sigma}{dy_W}(h_1 h_2 \rightarrow W^\pm X) &= K \frac{2\pi G_F}{3\sqrt{2}} x_1 x_2 \\ &\times \sum_{q,q'} |V_{qq'}|^2 [q(x_1, M_W^2) \bar{q}'(x_2, M_W^2) + \bar{q}'(x_1, M_W^2) q(x_2, M_W^2)]. \end{aligned} \quad (21)$$

In analogy the rapidity distribution for Z^0 boson is

$$\begin{aligned} \frac{d\sigma}{dy_Z}(h_1 h_2 \rightarrow Z^0 X) &= K \frac{8\pi G_F}{3\sqrt{2}} x_1 x_2 \sum_q [(g_V^q)^2 + (g_A^q)^2] \\ &\times [q(x_1, M_Z^2) \bar{q}(x_2, M_Z^2) + \bar{q}(x_1, M_Z^2) q(x_2, M_Z^2)], \end{aligned} \quad (22)$$

In the Eq. (21) and (22) the quark distributions must be evaluated at $x_{1/2} = \frac{M_B}{\sqrt{s}} e^{\pm y_B}$, where y_B is a rapidity of the produced W or Z boson.

The differential cross section for the production of charged leptons from the decay of W^\pm in the $h_1 h_2 \rightarrow W^\pm X \rightarrow l^\pm(\nu, \bar{\nu}) X \equiv l^\pm \tilde{X}$ can be easily calculated in the leading order approximation

$$\begin{aligned}
\frac{d\sigma}{dy_l}(h_1 h_2 \rightarrow W^\pm X \rightarrow l^\pm \tilde{X}) &= \frac{K}{3} \sum_{q,q'} \int_0^1 dx_1 dx_2 \\
&\times \left[q(x_1, M_W^2) \bar{q}'(x_2, M_W^2) \frac{d\sigma}{d\hat{y}_l}(q\bar{q}' \rightarrow W^\pm \rightarrow l^\pm l') \right. \\
&\left. + \bar{q}'(x_1, M_W^2) q(x_2, M_W^2) \frac{d\sigma}{d\hat{y}_l}(\bar{q}'q \rightarrow W^\pm \rightarrow l^\pm l') \right]. \quad (23)
\end{aligned}$$

In the equation above the lepton rapidity y_l is conventionally defined in the direction of h_1 . The cross section for the elementary $q\bar{q}' \rightarrow W^\pm \rightarrow l^\pm l'$ process is

$$\begin{aligned}
\frac{d\sigma}{d\hat{y}_l}(q\bar{q}' \rightarrow W^\pm \rightarrow l^\pm l') &= |V_{qq'}|^2 \left(\frac{G_F M_W^2}{4\sqrt{\pi}} \right)^2 \\
&\times \frac{\hat{s}}{(\hat{s} - M_W^2)^2 + (\Gamma_W M_W)^2} \left(\frac{1 \mp \tanh \hat{y}_l}{\cosh \hat{y}_l} \right)^2, \quad (24)
\end{aligned}$$

where $\hat{y}_l = y_l - \frac{1}{2} \ln(\frac{x_1}{x_2})$ and $\hat{s} = s x_1 x_2$.

The differential cross section for the production of charged leptons from the decay of Z^0 in the $h_1 h_2 \rightarrow Z^0 X \rightarrow l^+ l^- X \equiv l^+ \tilde{X}$ is

$$\begin{aligned}
\frac{d\sigma}{dy_l}(h_1 h_2 \rightarrow Z^0 X \rightarrow l^+ \tilde{X}) &= \frac{K}{3} \sum_q \int_0^1 dx_1 dx_2 \\
&\times \left[q(x_1, M_Z^2) \bar{q}(x_2, M_Z^2) \frac{d\sigma}{d\hat{y}_l}(q\bar{q} \rightarrow Z^0 \rightarrow l^+ l^-) \right. \\
&\left. + \bar{q}(x_1, M_Z^2) q(x_2, M_Z^2) \frac{d\sigma}{d\hat{y}_l}(\bar{q}q \rightarrow Z^0 \rightarrow l^+ l^-) \right]. \quad (25)
\end{aligned}$$

The cross section for the elementary $q\bar{q} \rightarrow Z^0 \rightarrow l^+ l^-$ is

$$\begin{aligned}
\frac{d\sigma}{d\hat{y}_l}(q\bar{q} \rightarrow Z^0 \rightarrow l^+ l^-) &= \left(\frac{G_F M_Z^2}{\sqrt{\pi}} \right)^2 \frac{\hat{s}}{(\hat{s} - M_Z^2)^2 + (\Gamma_Z M_Z)^2} \\
&\times \left\{ [(g_V^q)^2 + (g_A^q)^2] [(g_V^l)^2 + (g_A^l)^2] \right. \\
&\left. \times \left(\frac{1 \mp \tanh \hat{y}_l}{\cosh \hat{y}_l} \right)^2 \pm 8g_A^q g_V^q g_A^l g_V^l \frac{\tanh \hat{y}_l}{(\cosh \hat{y}_l)^2} \right\}. \quad (26)
\end{aligned}$$

As in the inclusive case the double integration over x_1 and x_2 can be reduced to a single integration over weak gauge boson rapidity in the “ δ -like” resonance approximation (20)

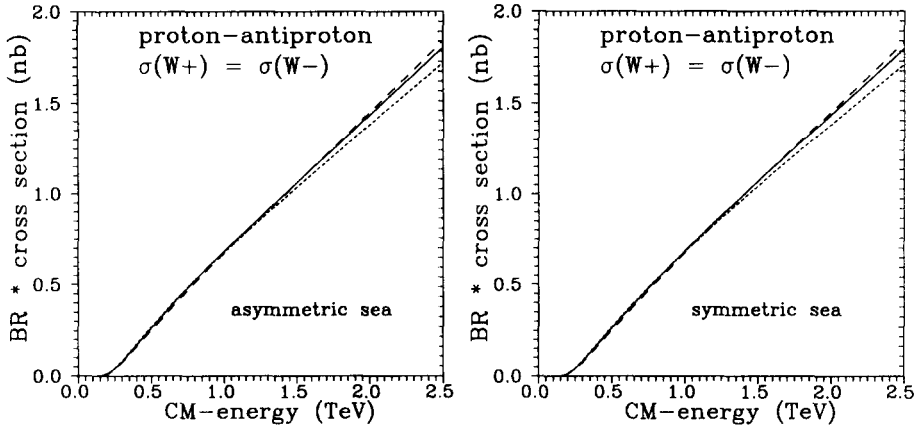


Fig. 3. The dependence of the total cross section times the electron decay branching ratio for the production of W ($W^+ + W^-$) in the proton-antiproton collisions on the value of $\Lambda_{\text{QCD}}^{(4)} = 150$ (dotted), 200 (solid) and 250 (dashed) MeV for model 1 and Model 2.

$$\begin{aligned}
 \frac{d\sigma}{dy_l}(h_1 h_2 \rightarrow W^\pm X \rightarrow l^\pm \bar{\nu}) &= K \sum_{q, q'} \int_{y_{\min}}^{y_{\max}} dy_W x_1 x_2 \\
 &\times \left[q(x_1, M_W^2) \bar{q}'(x_2, M_W^2) \frac{d\sigma}{d\hat{y}_l}(q \bar{q}' \rightarrow W^\pm \rightarrow l^\pm \nu(\bar{\nu})) \right. \\
 &\left. + \bar{q}'(x_1, M_W^2) q(x_2, M_W^2) \frac{d\sigma}{d\hat{y}_l}(\bar{q}' q \rightarrow W^\pm \rightarrow l^\pm \nu(\bar{\nu})) \right],
 \end{aligned}
 \tag{27}$$

where $y_{\min} = -\ln \frac{\sqrt{s}}{M_W}$, $y_{\max} = +\ln \frac{\sqrt{s}}{M_W}$.

In practical calculations we shall use $M_W = 80.22$ GeV, $\Gamma_W = 2.08$ GeV and $M_Z = 91.173$ GeV, $\Gamma_Z = 2.487$ GeV [33]. For a very recent review of experimental status see [34].

4. Results

The calculation of the cross sections for the gauge boson production (Eq. (21) and (22) or the cross section for the lepton from the gauge boson decay (Eq. (23) and (25)) requires knowledge of parton distributions at $Q^2 = M_W^2(M_Z^2)$. For this purpose the parton distributions found in Section 2 have been evolved by the Gribov–Lipatov–Altarelli–Parisi (GLAP) evolution equations [5]. In order to visualize uncertainty of running strong coupling constant in such an evolution, in Fig. 3 we have compared total cross sections for the W boson production obtained with three different values of $\Lambda_{\text{QCD}}^{(4)}$ (four active flavours) of 150 MeV (dotted), 200 MeV (solid), 250 MeV (dashed). In order to make a link to experimentally measured quantities the cross sections have been multiplied with appropriate branching ratio $\text{BR}(W^\pm \rightarrow e^\pm \nu(\bar{\nu}))$. In the heavy

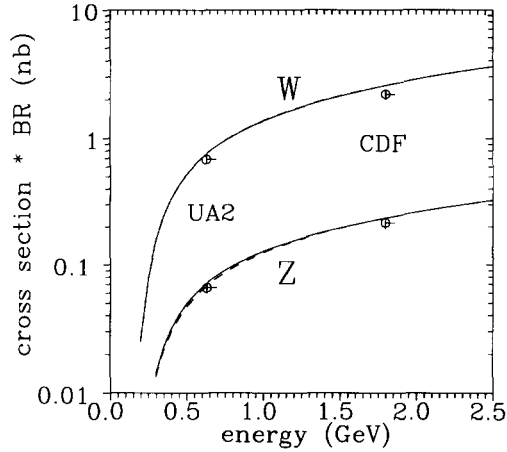


Fig. 4. Total cross section times the electron decay branching ratio for the production of W ($W^+ + W^-$) and Z^0 bosons in the proton–antiproton collisions compared with the experimental cross sections from the UA2 [37] and CDF [39] Collaborations. The solid line is a prediction of the model which explicitly includes the meson cloud corrections (Model 1), the dashed line represents a simple parametrization with $SU(2)$ symmetric nucleon sea (Model 2).

top-quark approximation $\text{BR}(W^\pm \rightarrow e^\pm \nu(\bar{\nu})) \approx \frac{1}{9}$. As seen from the figure, there is a 5–10% theoretical ambiguity on the level of the cross section at large $s^{1/2}$. The ambiguity practically cancels below $s^{1/2} = 1.2$ TeV. Since in the present paper we shall be interested mainly in relative effects (ratios, asymmetries), where the ambiguity due to the QCD evolution cancels almost completely, hereafter we shall limit to $\Lambda_{\text{QCD}}^{(4)} = 200$ MeV.

In order to test the sensitivity of our results to the gluon distribution we have varied the α_g and β_g parameters in Eq. (14) in the broad range. Only cross section at high energy ($s^{1/2} > 1$ TeV) shows some sensitivity to the gluon distribution. For instance at the Fermilab Tevatron energy, varying the α_g in the range 0 to 0.3 changes the total cross section by less than 2%. Similarly varying β_g by ± 1 modifies the total cross section by less than $\pm 2\%$. These variations are smaller than uncertainties due to the choice of Λ_{QCD} discussed above.

In Fig. 4 we compare energy dependence of the total cross section for the W and Z^0 production in the proton–antiproton collisions obtained with “Model 1” (solid line, with meson cloud, $\bar{u}-\bar{d}$ asymmetric sea) and “Model 2” (dashed line, without meson cloud, $\bar{u}-\bar{d}$ symmetric sea) with experimental data obtained by the UA2 [37] and CDF [39] Collaborations. In the heavy top-quark approximation

$$\text{BR}(Z^0 \rightarrow e^+e^-) \approx \frac{1 - 4x_W + 8x_W^2}{21 - 40x_W + \frac{160}{3}x_W^2}.$$

As seen from the figure the total cross section is not a good observable to distinguish between different models. In Table 2 in addition we compare the numerical values of the cross sections obtained in our model with those measured at CERN and Fermilab. A reasonable agreement of the total cross sections obtained within our model with those measured by UA1 [35], UA2 [36,37] and CDF [38,39] Collaborations can be seen.

Table 2

The total cross sections times branching ratio $\sigma_{\text{tot}}(p\bar{p} \rightarrow W^\pm X) \cdot \text{BR}(W^\pm \rightarrow e^\pm \nu(\bar{\nu}))$, $\sigma_{\text{tot}}(p\bar{p} \rightarrow Z^0 X) \cdot \text{BR}(Z^0 \rightarrow e^+ e^-)$ (in nb) for the production of W and Z bosons at CERN (upper block) and Fermilab (lower block)

Boson	Model 1	Model 2	Owens	GRV95(LO)	Experiment
$W^+ + W^-$	750.6	751.4	795.2	736.0	$682 \pm 12 \pm 40$ [37]
Z	71.7	68.2	74.5	70.0	$65.6 \pm 4.0 \pm 3.8$ [37]
$W^+ + W^-$	2548.0	2558.0	2298.0	2534.0	2200 ± 200 [39]
Z	234.1	233.1	218.6	236.6	214 ± 23 [39]

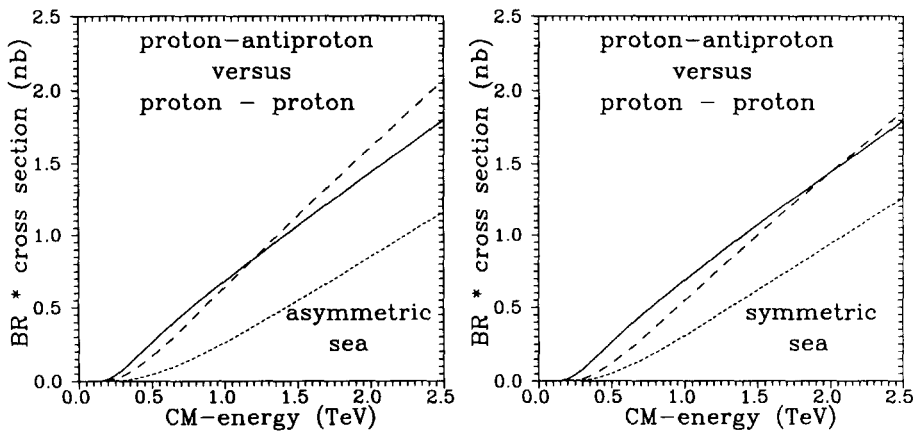


Fig. 5. A comparison of the total cross sections for the production of W -boson in the proton-proton (solid) and proton-antiproton (dashed) collisions. In panel (a) we show the results for the asymmetric sea induced by the meson cloud and in panel (b) the results for the symmetric sea quark parametrization.

Naively one would expect that the total cross section for the production of gauge W bosons should be smaller in the proton-proton collisions than in the proton-antiproton collisions, because in the latter case the antiproton is an efficient donor of antiquarks. This was used in the past as a strong argument for the construction of proton-antiproton colliders such as those at CERN and Fermilab. Since at that time it was strongly believed that the nucleon sea is symmetric with respect to the light flavours, no $\bar{d} \neq \bar{u}$ scenario has been considered. At present there are fairly convincing arguments [4,12] for the $\bar{d}-\bar{u}$ asymmetry. Can the $\bar{d}-\bar{u}$ asymmetry induced by the meson cloud in the nucleon modify this simple expectation? In Fig. 5a we compare the proton-proton and proton-antiproton cross sections for the “asymmetric” (panel a) and “symmetric” (panel b) sea. The corresponding cross sections are denoted as: $\sigma_{\text{tot}}(p\bar{p} \rightarrow W^+) = \sigma_{\text{tot}}(p\bar{p} \rightarrow W^-)$ (solid), $\sigma_{\text{tot}}(pp \rightarrow W^+)$ (dashed) and $\sigma_{\text{tot}}(pp \rightarrow W^-)$ (dotted). As expected, without meson cloud, with symmetric sea quark distributions, the cross section for the production of W^+ is smaller in the proton-proton case than in the proton-antiproton case. In contrast, much larger cross sections are obtained if the meson cloud effects are included (see panel a). As seen from the figure, in the broad range of energy $\sigma_{\text{tot}}(pp \rightarrow W^+) > \sigma_{\text{tot}}(p\bar{p} \rightarrow W^+) = \sigma_{\text{tot}}(p\bar{p} \rightarrow W^-)$. In Fig. 6 we show an enhancement factor

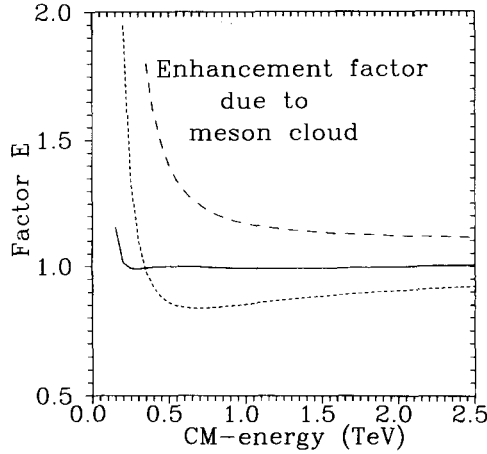


Fig. 6. The enhancement factors $E_{W^+}^{pp}$ (dashed line), $E_{W^-}^{pp}$ (dotted line) and $E_W^{p\bar{p}}$ (solid line).

of the cross sections due to the meson cloud effects defined as

$$E_{W^\pm}^{pp} \equiv \frac{\sigma_{\text{tot}}(pp \rightarrow W^\pm, \text{asymmetric})}{\sigma_{\text{tot}}(pp \rightarrow W^\pm, \text{symmetric})},$$

$$E_{W^\pm}^{p\bar{p}} \equiv \frac{\sigma_{\text{tot}}(p\bar{p} \rightarrow W^\pm, \text{asymmetric})}{\sigma_{\text{tot}}(p\bar{p} \rightarrow W^\pm, \text{symmetric})}. \quad (28)$$

$E_{W^+}^{pp}$ (dashed line), $E_{W^-}^{pp}$ (dotted line) and $E_{W^+}^{p\bar{p}} = E_{W^-}^{p\bar{p}}$ (solid line) are shown in Fig. 6. A huge enhancement of the cross section due to the meson cloud effects close to the threshold can be observed in the proton–proton collision case. In principle this effect could be studied in the future at the heavy-ion collider RHIC. There is practically no such enhancement in the proton–antiproton collision case, except very close to the threshold, where the corresponding cross section is negligibly small.

A very interesting quantity is the asymmetry of charged leptons from $W^\pm \rightarrow l^\pm(\nu, \bar{\nu})$ decays defined as

$$A_{p\bar{p}}^{l^+l^-}(y_l) = \frac{\frac{d\sigma}{dy_l}(p\bar{p} \rightarrow W^+X \rightarrow l^+\tilde{X}) - \frac{d\sigma}{dy_l}(p\bar{p} \rightarrow W^-X \rightarrow l^-\tilde{X})}{\frac{d\sigma}{dy_l}(p\bar{p} \rightarrow W^+X \rightarrow l^+\tilde{X}) + \frac{d\sigma}{dy_l}(p\bar{p} \rightarrow W^-X \rightarrow l^-\tilde{X})}. \quad (29)$$

The quantity has been measured recently by the CDF Collaboration at the Fermilab $p\bar{p}$ Tevatron collider [40,41]. The experimental results [41] (open circles) together with results of different calculations specified below, are shown in Fig. 7. New preliminary CDF data [42] are shown in Fig. 7 by the solid triangles. The experimental data have been folded across $y_l = 0$ by the CDF Collaboration [41] based on the CP invariance. In the calculation experimental cut [41] $p_{T,\text{min}}^l = 25$ GeV has been applied which, as will be discussed later, is of crucial importance. In panel (a) we show asymmetries obtained in our Model 1 (solid line) and Model 2 (dashed line). As clearly seen from the figure the presence of the meson cloud considerably improves the agreement with the experimental asymmetry. A similar quality agreement with the CDF asymmetry has been

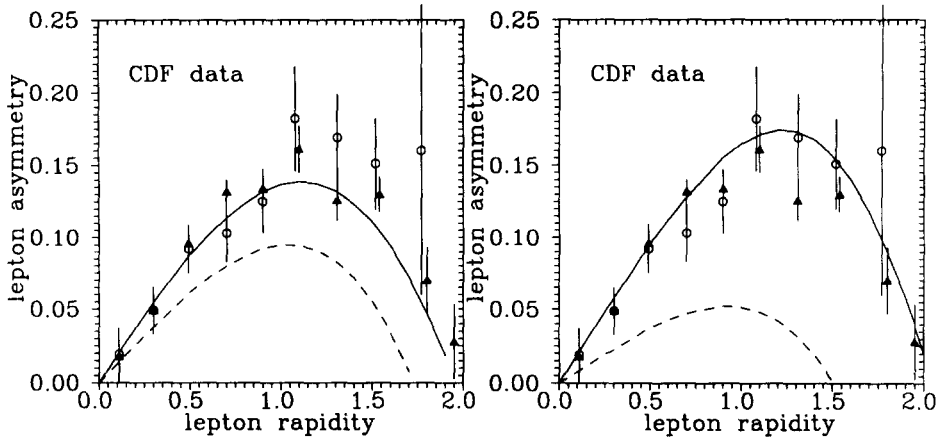


Fig. 7. Predictions for the asymmetry $A_{pp}^{e^+e^-}$ of the rapidity distributions of the charged leptons from the $W^\pm \rightarrow l^\pm \nu$ decays in the proton-antiproton collisions. The results of Model 1 (solid) and Model 2 (dashed) are shown in panel (a). For comparison in panel (b) we show lepton asymmetries calculated with the GRV95(LO) [44] (solid) and Owens [45] (dashed) parametrizations of quark distributions. The published CDF experimental data [41] are shown by the open circles and the new preliminary CDF data [42] by the full triangles.

achieved recently in Ref. [43] where the quark distributions from a recent “radiative” parametrization of quark distributions by Glück-Reya-Vogt (GRV) [44] have been used. While in Ref. [44] the $\bar{d}-\bar{u}$ asymmetry was introduced purely phenomenologically, in the present paper the $\bar{d}-\bar{u}$ asymmetry is ascribed to the effects caused by the meson cloud in the nucleon. For comparison in panel (b) we show the asymmetry obtained with the recent GRV parametrization of quark distributions [44] (solid line) and somewhat older parametrization of Owens [45] (dashed line). The curves in panel (b) remind very much those in panel (a). While in the Owens parametrization the sea was assumed to be $SU(3)$ -symmetric ($u_s = \bar{u}_s = d_s = \bar{d}_s = s_s = \bar{s}_s$), the assumption was relaxed in the GRV parametrization where both $SU(3)$ and $SU(2)$ symmetry violation effects in the nucleon sea were included in a pseudo-fit to DIS experimental data [44]. The similarity of panel (a) and panel (b) strongly suggest that the $\bar{d}-\bar{u}$ asymmetry is fairly important to understand the leptonic asymmetry $A_{pp}^{e^+e^-}(y_e)$.

In order to better understand the lepton asymmetry shown in Fig. 7, in Fig. 8 we present the gauge boson asymmetry (dotted line) defined as

$$A_{pp}^{W^+W^-}(y_W) = \frac{\frac{d\sigma}{dy_W}(p\bar{p} \rightarrow W^+X) - \frac{d\sigma}{dy_W}(p\bar{p} \rightarrow W^-X)}{\frac{d\sigma}{dy_W}(p\bar{p} \rightarrow W^+X) + \frac{d\sigma}{dy_W}(p\bar{p} \rightarrow W^-X)}. \quad (30)$$

Almost full asymmetry $|A_{pp}^{W^+W^-}| = 1$ is reached at large $|y_W| \approx 3$. For completeness we show also the lepton asymmetry $A_{pp}^{e^+e^-}$ without any experimental cuts (dashed line) and with the experimental cuts (solid line). A huge dilution in comparison to the W-boson asymmetry $A_{pp}^{W^+W^-}$ can be observed. As seen by a comparison of the dashed (no cuts) and solid (with cuts) lines, experimental effects increase the asymmetry considerably,

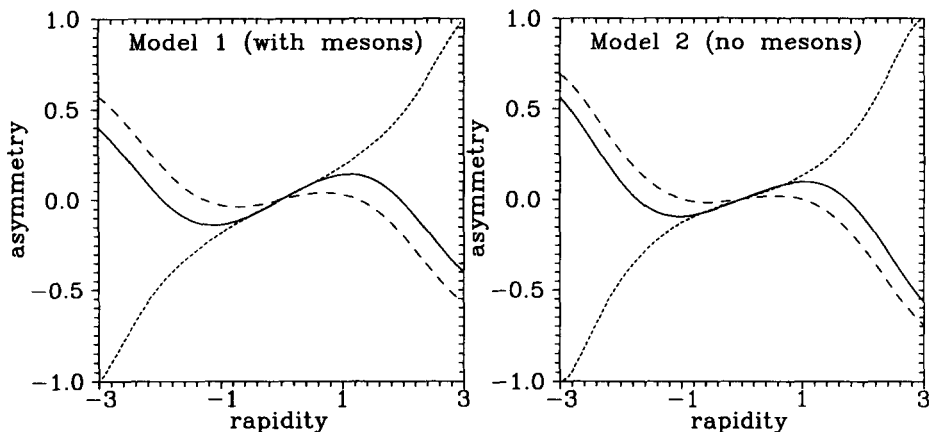


Fig. 8. The boson asymmetry $A_{pp}^{W^+W^-}(y_W)$ (dotted line), the lepton asymmetry $A_{pp}^{e^+e^-}(y_e)$ without experimental cuts (dashed line) and with experimental cuts (solid line). The results obtained in Model 1 (panel a) are compared with those in Model 2 (panel b).

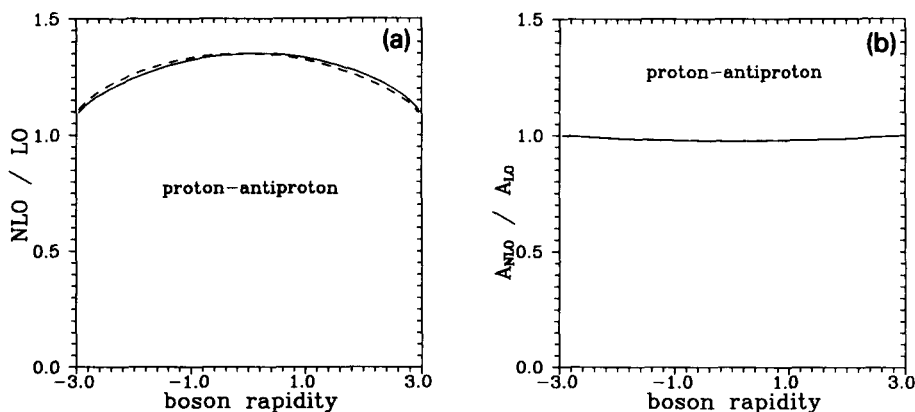


Fig. 9. (a) The ratio of the NLO/LO cross sections as a function of y_{W^+} (solid) and y_{W^-} (dashed) cross section. (b) The ratio of the NLO/LO gauge boson asymmetries $A_{pp}^{W^+W^-}$ as a function of y_W .

improving agreement with the CDF experimental data [41]. It has been checked that uncertainties of parameters in the gluon distribution cancel almost completely for boson and lepton asymmetries of rapidity distributions discussed above. The same stay true for all asymmetries which are discussed below.

Let us come back now to the problem of accuracy of the leading order approximation. In Fig. 9a we present a ratio of NLO/LO cross sections as a function of boson W^+ (solid line) and W^- (dashed line) rapidities. The NLO corrections lead to a rapidity dependent enhancement $K(y_W)$ over the leading order result. At $y_W \approx 0$, where most of the cross section is concentrated, the enhancement is approximately the same as given by the approximate K -factors from the previous section. At larger $|y_W|$ the approximation of constant K -factors is not sufficient. However, because the $K(y_W)$ functions are to a good approximation the same for W^+ and W^- (compare solid and dashed line in

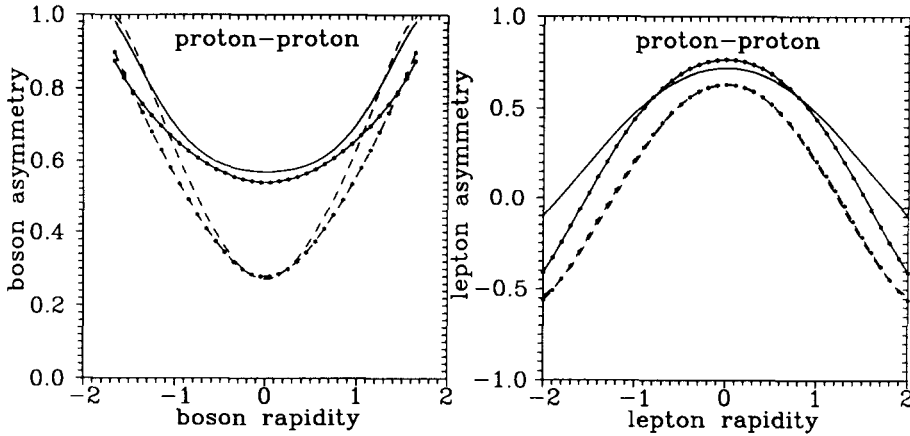


Fig. 10. $A_{pp}^{W^+W^-}$ (panel a) and corresponding $A_{pp}^{e^+e^-}$ (panel b). The asymmetries obtained in Model 1 (solid line) and Model 2 (dashed line) are compared with the results obtained with the GRV95(LO) parametrization [44] (solid line with dots) and the Owens parametrization [45] (dashed line with dots).

Fig. 9a) the predicted LO and NLO asymmetries are within 4% the same (see Fig. 9b). This advantageous situation allows to study the interesting non-perturbative effects of the meson cloud in much simpler QCD leading order approximation where the parton distributions have in addition much simpler interpretation (in the NLO analysis parton distributions must be redefined to absorb mass and infrared singularities). The conclusion found here stays true for all other asymmetries studied in the rest of this paper.

Having shown that our parton distributions lead to a good description of DIS data at relatively low Q^2 and describe the gauge bosons production data in the proton-antiproton collisions fairly well, we shall try to make some interesting predictions for the W/Z production in nucleon-nucleon collisions, which could be measured in principle at the future collider RHIC originally designed to study the quark-gluon plasma in heavy ion - heavy ion collisions. The option to study the proton - proton collisions has been analysed only recently.

In the following we shall fix the energy $s^{1/2}$ to 500 GeV which could be roughly adequate for the proton-proton collisions at RHIC. In Fig. 10 we present $A_{pp}^{W^+W^-}$ (panel a) and in analogy to the proton-antiproton case $A_{pp}^{e^+e^-}$ (panel b). Let us demonstrate that $A_{pp}^{W^+W^-}$ is a quantity sensitive to the $\bar{u}-\bar{d}$ asymmetry. For this purpose let us write

$$\begin{aligned}\bar{u}(x, Q^2) &= S(x, Q^2) - \frac{\Delta(x, Q^2)}{2}, \\ \bar{d}(x, Q^2) &= S(x, Q^2) + \frac{\Delta(x, Q^2)}{2}.\end{aligned}\quad (31)$$

Then taking $y_W \approx 0$ ($x_1 \approx x_2$) and neglecting small (Cabibbo suppressed) contributions from the strange quarks, the asymmetry $A_{pp}^{W^+W^-}$ can be written as

$$A_{pp}^{W^+W^-}(x) \approx \frac{R_v(x)S(x) + \frac{\Delta(x)}{2}}{S(x) + R_v(x)\frac{\Delta(x)}{2}}, \quad (32)$$

where we have introduced $R_v(x) \equiv \frac{u_v(x) - d_v(x)}{u_v(x) + d_v(x)}$ for brevity. Eq. (32) clearly demonstrates the sensitivity to the \bar{u} - \bar{d} asymmetry which in our model is due to the meson cloud effects. The sensitivity to the \bar{u} - \bar{d} difference can be better visualized in the ratio

$$R_{pp}^{W^+W^-} \equiv \frac{\sigma(pp \rightarrow W^+X)}{\sigma(pp \rightarrow W^-X)}. \quad (33)$$

With the same approximations as above

$$R_{pp}^{W^+W^-} \approx \frac{u(x, M_W^2)}{d(x, M_W^2)} \frac{\bar{d}(x, M_W^2)}{\bar{u}(x, M_W^2)}. \quad (34)$$

The first ratio is known fairly well from the CDF data (see for instance Ref. [25]). Therefore the measurement of $R_{pp}^{W^+W^-}(x = M_W/\sqrt{s})$ in p+p collision should give an accurate determination of the ratio $\bar{d}(x, M_W^2)/\bar{u}(x, M_W^2)$. For a typical RHIC energy $s^{1/2} = 500$ GeV, $x \approx 0.16$. This is a region of sizeable \bar{u} - \bar{d} asymmetry. Analogous ratio has been determined recently at $Q^2 \approx 20$ GeV² from the measurement of Drell-Yan asymmetry in proton-proton and proton-deuteron collisions by the NA51 experiment at CERN [4]. There, however, the $\bar{u}(x)/\bar{d}(x)$ is biased by the explicit assumption about proton-neutron isospin symmetry [12]. In contrast, $R_{pp}^{W^+W^-}(x)$ is free of such an assumption. It is not fully clear at present how good the proton-neutron isospin symmetry actually is on the level of parton distributions. Therefore any independent verification, free of explicit assumption of proton-neutron isospin symmetry, would be very useful.

In analogy to the Drell-Yan asymmetries used in Refs. [4,12] and asymmetries defined by Eq. (30) and Eq. (29) we shall consider now some new asymmetries $A_{pp,pn}^B$ and $A_{pp,pn}^l$ for the proton-proton and proton-neutron scattering defined as

$$A_{pp,pn}^B(y_B) = \frac{\frac{d\sigma}{dy_B}(pp \rightarrow BX) - \frac{d\sigma}{dy_B}(pn \rightarrow BX)}{\frac{d\sigma}{dy_B}(pp \rightarrow BX) + \frac{d\sigma}{dy_B}(pn \rightarrow BX)}. \quad (35)$$

and

$$A_{pp,pn}^l(y_l) = \frac{\frac{d\sigma}{dy_l}(pp \rightarrow BX \rightarrow l\tilde{X}) - \frac{d\sigma}{dy_l}(pn \rightarrow BX \rightarrow l\tilde{X})}{\frac{d\sigma}{dy_l}(pp \rightarrow BX \rightarrow l\tilde{X}) + \frac{d\sigma}{dy_l}(pn \rightarrow BX \rightarrow l\tilde{X})}. \quad (36)$$

In the definitions above B represents W^+ , W^- or Z^0 bosons and l can be any charged lepton. In Fig. 11 we present $A_{pp,pn}^{W^\pm}$ (panel a) and corresponding $A_{pp,pn}^{e^\pm}$ (panel b). For the sake of completeness in Fig. 12 we present $A_{pp,pn}^{Z^0}$ (panel a) and corresponding $A_{pp,pn}^{e^\pm}$ (panel b).

An interesting observations can be made by a careful inspection of Figs. 10–12. In general, the calculated lepton asymmetries are rather different from corresponding gauge boson asymmetries. In all the cases considered the results can be classified into two distinct groups:

- (a) results obtained with quark distributions possessing \bar{d} - \bar{u} asymmetry (our Model 1, where the meson cloud effects are explicitly included and GRV95(LO) parametrization [44]),

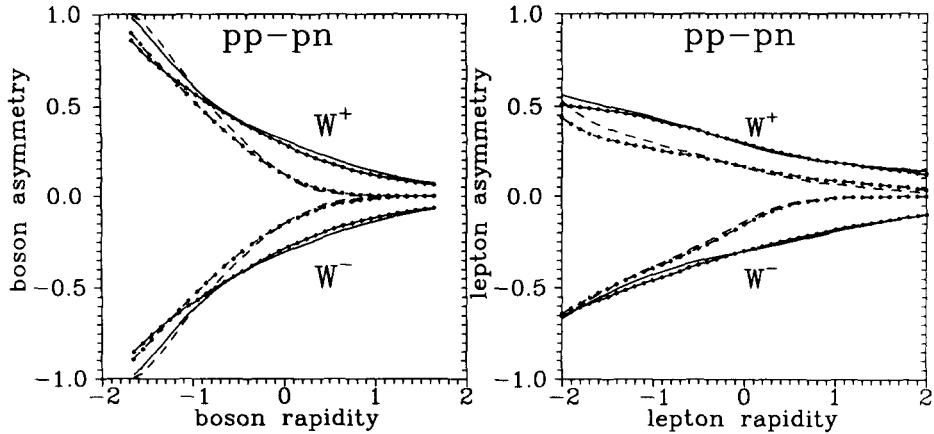


Fig. 11. $A_{pp,pn}^W$ (panel a) and corresponding $A_{pp,pn}^e$ (panel b). The result for the W^+ (e^+) and W^- (e^-) are shown together in the upper and lower parts of the diagrams, respectively. The asymmetries obtained in Model 1 (solid line) and Model 2 (dashed line) are compared with the results obtained with the GRV95(LO) parametrization [44] (solid line with dots) and the Owens parametrization [45] (dashed line with dots).

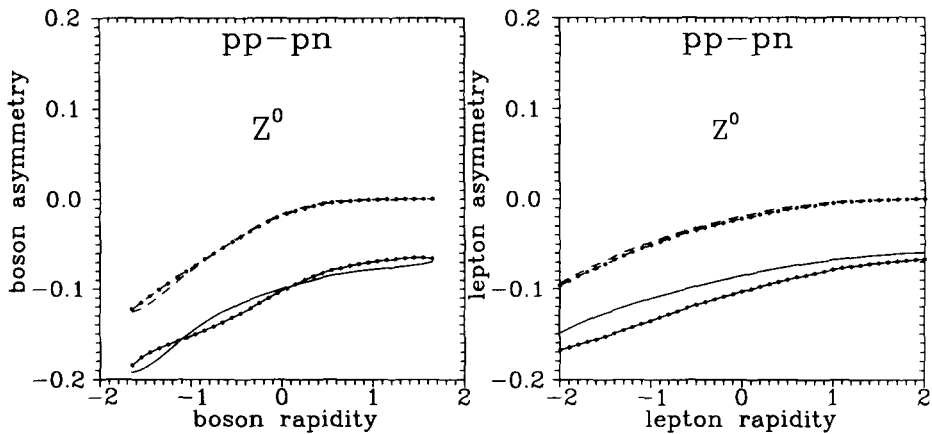


Fig. 12. $A_{pp,pn}^Z$ (panel a) and corresponding $A_{pp,pn}^e$ (panel b). The asymmetries obtained in Model 1 (solid line) and Model 2 (dashed line) are compared with the results obtained with the GRV95(LO) parametrization [44] (solid line with dots) and the Owens parametrization [45] (dashed line with dots).

(b) results obtained with $SU(2)$ symmetric quark distributions (our Model 2 and Owens parametrization [45]).

The measuring of such quantities in the future would be therefore of great help in studying the asymmetry of the sea quark distributions in the nucleon, which seems mandatory in better understanding of the nucleon structure. Whether such an analysis will be possible in the future at the heavy-ion collider RHIC requires new studies of several experimental aspects. We find a possible option to extend in a further future the investigation of the (heavy ion) –(heavy ion) collisions to more elementary proton–proton and proton–deuteron collision a very interesting possibility.

5. Conclusions

The concept of the meson cloud in the nucleon was found recently to be very useful [10,12] in understanding the Gottfried Sum Rule violation observed by the New Muon Collaboration [2] and the Drell–Yan asymmetry measured recently in the NA51 Drell–Yan experiment at CERN [4]. In the present paper we have investigated possible effects of the meson cloud in the nucleon on the production of weak gauge bosons in proton–antiproton, proton–proton and proton–deuteron collisions.

In order to get reliable results for the gauge boson production we have started our analysis from the description of deep-inelastic structure functions measured in both muon and (anti)neutrino charged current DIS. The meson cloud corrections have been calculated explicitly. Although the structure of the bare nucleon (undressed of the meson cloud) is presumably much simpler than that of the physical nucleon, its structure function cannot be calculated at present from first principles. In order to get a good description of the lepton DIS data the quark distributions in the bare nucleon have been fitted, including *parameter free* meson cloud corrections (Model 1). For comparison we have made our own fit to DIS data neglecting meson cloud effects (Model 2). In both cases the dominant kinematical effect of target mass corrections have been included. The inclusion of the target mass corrections turned out to be fairly important for the charged lepton asymmetry measured by the CDF Collaboration [41].

The calculation of the cross sections for the weak gauge boson production requires parton distributions at $Q^2 = M_W^2 (M_Z^2)$. For this purpose the parton distributions at low Q^2 have been evolved by the Gribov–Lipatov–Altarelli–Parisi evolution equations.

A reasonable agreement of the total cross sections calculated with so-obtained parton distributions with those measured at CERN by the UA1 [35], UA2 [36,37] Collaborations and at Fermilab by the CDF [38,39] Collaboration has been obtained. If the meson cloud effects are included in the broad range of energy $\sigma_{\text{tot}}(pp \rightarrow W^+) > \sigma_{\text{tot}}(p\bar{p} \rightarrow W^+) = \sigma_{\text{tot}}(p\bar{p} \rightarrow W^-)$, in contrast to naive expectations. In contrast to parton distributions with $SU(2)$ symmetric sea we find a good description of the charged lepton asymmetry measured recently by the CDF Collaboration [41] which may be treated as an indirect evidence of the meson cloud in the nucleon.

Having shown that our parton distributions lead to a good description of DIS data at low Q^2 and describe well the gauge bosons production data in proton–antiproton collisions, we have analysed some asymmetries of the cross sections for the production of W/Z bosons in the proton–proton and proton–deuteron collisions. We find that such observables can be very useful to shed new light on the problem of the $\bar{d}-\bar{u}$ asymmetry in the nucleon. These quantities could in principle be studied in the future at the heavy ion collider RHIC. Whether such an analysis will be possible in practice will require, however, new studies of several experimental aspects.

Acknowledgements

One of us (A.S.) is indebted to Stefan Kretzer for a detailed discussion concerning Ref. [43] and James Stirling for discussion concerning target mass corrections. We are also indebted to Arie Bodek and Paweł de Barbaro for providing us with new preliminary CDF data on the charged lepton asymmetry in proton–antiproton collision.

References

- [1] K. Gottfried, Phys. Rev. Lett. 18 (1967) 1174.
- [2] P. Amaudruz et al., Phys. Rev. Lett. 66 (1991) 2712.
- [3] M. Arneodo et al., Phys. Rev. D 50 (1994) R1.
- [4] A. Baldit et al., Phys. Lett. B 332 (1994) 244.
- [5] G. Altarelli and G. Parisi, Nucl. Phys. B 126 (1977) 298.
- [6] D.A. Ross and C.T. Sachrajda, Nucl. Phys. B 149 (1979) 497.
- [7] R.D. Field and R.P. Feynman, Phys. Rev. D 15 (1977) 259.
- [8] F. Buccella and J. Soffer, Europhys. Lett. 24 (1993) 165;
F. Buccella and J. Soffer, Phys. Rev. D 93 (1993) 5416;
F. Buccella and J. Soffer, Mod. Phys. Lett. A 8 (1993) 225;
C. Bourrely, F. Buccella, G. Miele, G. Migliore, J. Soffer and V. Tibullo, Z. Phys. C 62 (1994) 431;
F. Buccella, G. Miele, G. Migliore and V. Tibullo, Z. Phys. C 68 (1995) 631.
- [9] E.M. Henley and G.A. Miller, Phys. Lett. B 251 (1990) 453;
A. Signal, A.W. Schreiber and A.W. Thomas, Mod. Phys. Lett. A 6 (1991) 271;
S. Kumano, Phys. Rev. D 43 (1991) 59;
W.-Y.P. Hwang, J. Speth and G.E. Brown, Z. Phys. A 339 (1991) 383;
A. Szczurek and J. Speth, Nucl. Phys. A 555 (1993) 249;
A. Szczurek, J. Speth and G.T. Garvey, Nucl. Phys. A 570 (1994) 765.
- [10] H. Holtmann, A. Szczurek and J. Speth, Nucl. Phys. A 596 (1996) 631.
- [11] H. Holtmann, N.N. Nikolaev, J. Speth and A. Szczurek, Z. Phys. A 353 (1996) 411.
- [12] A. Szczurek, M. Ericson, H. Holtmann and J. Speth, Nucl. Phys. A 596 (1996) 397.
- [13] Z. Dziembowski, H. Holtmann, A. Szczurek and J. Speth, submitted to Phys. Lett. B;
Z. Dziembowski, H. Holtmann, A. Szczurek and J. Speth, submitted to Annals of Physics (N.Y.).
- [14] J.C. Peng and D.M. Jansen, Phys. Lett. B 354 (1995) 460.
- [15] V.R. Zoller, Z. Phys. C 53 (1992) 443.
- [16] J.D. Sullivan, Phys. Rev. D 5 (1972) 1732.
- [17] P.J. Sutton, A.D. Martin, R.G. Roberts and W.J. Stirling, Phys. Rev. D 45 (1992) 2349.
- [18] W.-Y.P. Hwang and J. Speth, Phys. Rev. D 46 (1992) 1198.
- [19] H. Georgi and H.D. Politzer, Phys. Rev. 14 (1976) 1829.
- [20] F.J. Yndurain, The Theory of Quark and Gluon Interactions (Springer, Berlin, 1993).
- [21] A.D. Martin, W.J. Stirling and R.G. Roberts, Phys. Rev. 51 (1995) 4756.
- [22] W.C. Leung et al., Phys. Lett. B 317 (1993) 655.
- [23] S.R. Mishra et al., Phys. Rev. Lett. 68 (1992) 3499.
- [24] C. Foudas et al., Phys. Rev. Lett. 64 (1990) 1207.
- [25] A.D. Martin, W.J. Stirling and R.G. Roberts, Phys. Rev. D 50 (1994) 6734. A.D. Martin, R.G. Roberts and W.J. Stirling, Phys. Lett. B 387 (1996) 419.
- [26] J. Botts, J.G. Morfin, J.F. Owens, J. Qiu, W.K. Tung and H. Weerts, Phys. Lett. B 304 (1993) 159;
H.L. Lai, J. Botts, J. Huston, J.G. Morfin, J.F. Owens, J.W. Qiu, W.K. Tung and H. Weerts, Phys. Rev. D 51 (1995) 4763;
H.L. Lai, J. Huston, S. Kuhlmann, F. Olness, J. Owens, D. Soper, W.K. Tung, H. Weerts, Phys. Rev. D 55 (1997) 1280.
- [27] M. Glück, E. Reya and A. Vogt, Z. Phys. C 67 (1995) 433.
- [28] M. Derrick et al. (ZEUS), Phys. Lett. B 384 (1996) 388.

- [29] A. Szczurek and A. Budzanowski, in print in Phys. Lett. B.
- [30] F. Abe et al. (CDF), Phys. Rev. Lett. 77 (1996) 438.
- [31] W.T. Giele, E.W.N. Glover and D.A. Kosower, Nucl. Phys. B 403 (1993) 633.
- [32] V.D. Barger and R.J.N. Philips, Collider Physics (Addison-Wesley, Redwood City, 1987).
- [33] Review of Particle Properties, Phys. Rev. D 45 (1992) 1.
- [34] S.E. Kopp, Int. Jour. Mod. Phys. A 10 (1995) 4413.
- [35] C. Albajar et al. (UA1 Collaboration), Phys. Lett. B 253 (1991) 503.
- [36] J. Alitti et al. (UA2 Collaboration), Z. Phys. C 47 (1990) 11.
- [37] J. Alitti et al. (UA2 Collaboration), Phys. Lett. B 276 (1992) 365.
- [38] F. Abe et al. (CDF Collaboration), Phys. Rev. D 44 (1991) 29.
- [39] F. Abe et al. (CDF Collaboration), Phys. Rev. Lett. 69 (1992) 28.
- [40] F. Abe et al. (CDF Collaboration), Phys. Rev. Lett. 68 (1992) 1459.
- [41] F. Abe et al. (CDF Collaboration), Phys. Rev. Lett. 74 (1995) 850.
- [42] A. Bodek, a talk given at the third Int. Symp. on Radiative Corrections, Cracow, Poland, August 1–5, 1996.
- [43] S. Kretzer, E. Reya and M. Stratmann, Phys. Lett. B 348 (1995) 628.
- [44] M. Glück, E. Reya and A. Vogt, Z. Phys. C 67 (1995) 433.
- [45] J.F. Owens, Phys. Lett. B 266 (1991) 126.